# NON-LINEAR INSTABILITY OF PERIODIC ORBITS OF SUSPENSIONS OF THIN FIBERS IN FLUIDS

STEPHEN MONTGOMERY-SMITH

Abstract. It is known that Jeffery's equation predicts that fibers with Jeffery's parameter less than one will exhibit periodic behavior when subjected to shear flows. Yet this behavior is not seen in suspensions containing many fibers. This paper explores the extent to which coupling Jeffery's equation with the viscosity of the suspension causes instability that breaks up this periodic behavior. A simple one-dimensional model is presented, which suggests that there is at least some non-linear instability, so that this may at least partially account for why periodic behavior is not observed. One interesting observation is that this instability only grows linearly if only two dimensions are considered, whereas the instability can have exponential growth if the third dimension is considered.

## 1. Introduction

Predicting the orientation of thin fibers suspended in fluid flows with low Reynolds number finds many industrial applications, for example, in creating parts using injection molded plastics. One method that has been widely used is to start with the assumption that Jeffery's equation (Jeffery, 1923), or some variation of it, is a good predictor of the orientation of the fibers. Jeffery's equation alone has been seen to be a poor predictor of the behavior of fibers in fluids when the volume ratio of fibers is reasonably high. It is clear that hydrodynamic interactions between the fibers have a very important effect. One way hydrodynamic effects are modeled is by including diffusion terms to Jeffery's equation (Bird *et al.*, 1987), for example, the Folgar-Tucker equation (Folgar & Tucker, 1984).

In Montgomery-Smith (2011), a different mechanism for accounting for hydrodynamic interactions was proposed. Jeffery's equation was coupled with an anisotropic version of Stokes' equation, where the relationship between the stress and the strain depended upon the orientation of the fibers. Formulas and software to analyze the linearization of perturbations of a uniform fiber distribution were developed. In this paper we will consider non-linear perturbations of this same system of equations in a special case when the numeric calculations are easy to perform, that is, a shear flow when the fiber orientation is a function only of one coordinate. We refer to this special case as a *one-dimensional model*, as the resulting PDE is in one spacial variable only.

This paper concentrates on one aspect of how experimental data differs from the pure Jeffery's equation. Jeffery's equation for fibers with finite aspect ratio ($|\lambda| < 1$) predicts that under a shear flow, the fiber orientation is periodic in time, with period $4\pi/\sqrt{1-\lambda^2}$ divided by shear rate. (The $4\pi$ is replaced by $2\pi$ if the fiber orientation has certain symmetries.) We show this periodicity in the left hand side graphs of Figures 2 and 4 showing the force required to maintain constant shear rate, and in the left hand side graphs of Figures 3 and 5 showing components of the second moment tensor of the fiber orientation. This is referred

to as Jeffery's 'tumbling,' and is not seen in experiments (see, for example, Anczurowski & Mason, 1967).

## 2. The coupled Jeffery-Stokes Equation

The version of Jeffery's equation we use solves for $\psi$, the probability distribution of the orientation of fibers, at each point in time and space. This is a function $\psi(\mathbf{x}, \mathbf{p}, t)$ of the three variables: space $\mathbf{x} = (x, y, z)$, time $t$, and orientation $\mathbf{p} \in S$, where $S = \{\mathbf{p} = (p_1, p_2, p_3) : p_1^2 + p_2^2 + p_3^2 = 1\}$ is the two dimensional sphere. Note the isotropic distribution is given by $\psi = 1/4\pi$. The equations involve the velocity field $\mathbf{u} = (u_1, u_2, u_3)$, which is a function of space $\mathbf{x}$ and time $t$. Associated with the velocity field $\mathbf{u}$ are the Jacobian matrix $\boldsymbol{\nabla}\mathbf{u} = [\partial u_i/\partial x_j]_{1\le i,j\le 3}$, the deformation matrix or rate of strain tensor $\mathsf{\Gamma} = \boldsymbol{\nabla}\mathbf{u} + (\boldsymbol{\nabla}\mathbf{u})^T$, and the vorticity matrix $\Omega = \boldsymbol{\nabla}\mathbf{u} - (\boldsymbol{\nabla}\mathbf{u})^T$. Jeffery's equation is

$$\frac{\partial \psi}{\partial t} + \mathbf{u}\cdot\boldsymbol{\nabla}\psi = -\tfrac{1}{2}\boldsymbol{\nabla}_{\mathbf{p}}\cdot((\Omega\cdot\mathbf{p} + \lambda(\mathsf{\Gamma}\cdot\mathbf{p} - \mathsf{\Gamma} : \mathbf{ppp}))\psi) \tag{1}$$

Here $\boldsymbol{\nabla}_{\mathbf{p}}$ denotes the gradient on the sphere $S$.

The model that was proposed in Montgomery-Smith (2011) was to couple Jeffery's equation with how the fiber orientation effects the viscosity of the suspension. It is stated in Batchelor (1971); Shaqfeh & Fredrickson (1990) that if the underlying fluid is Newtonian, then the stress-strain relation for slender fibers is

$$\tau = \nu(\beta(\mathbb{A} : \mathsf{\Gamma} - \tfrac{1}{3}\mathsf{I}(\mathsf{A} : \mathsf{\Gamma})) + \mathsf{\Gamma}) - p\mathsf{I} \tag{2}$$

Here $\tau$ is the stress tensor, $\mathsf{A}$ and $\mathbb{A}$ are respectively the the 2nd and 4th moment tensors

$$\mathsf{A} = \int_S \mathbf{pp}\,\psi\,d\mathbf{p} \tag{3}$$

$$\mathbb{A} = \int_S \mathbf{pppp}\,\psi\,d\mathbf{p} \tag{4}$$

$\nu$ is the Newtonian viscosity that the underlying fluid would have if the fibers were absent (without loss of generality we set $\nu = 1$), $p$ is the pressure, and $\beta$ is a dimensionless quantity that is related to the volume fraction of the fibers in the fluid. The quantity $\beta$ represents the extent to which fibers act as 'stiffeners' to the fluid motion. The paper Sepehr *et al.* (2004) suggests that the order of magnitude of $\beta$ could easily be as large as 50 or 100.

We assume that the velocity field obeys the following incompressible Stokes' equation:

$$\boldsymbol{\nabla}\cdot\tau = 0 \tag{5}$$

$$\boldsymbol{\nabla}\cdot\mathbf{u} = 0 \tag{6}$$

Since the fluid is incompressible, the pressure $p$ is obtained implicitly, and hence without changing any of the results, we can replace $\frac{1}{3}\beta\mathsf{A} : \Gamma + p$ by a single scalar $q$, so that the stress-strain equation becomes

$$\tau = \beta\mathbb{A} : \mathsf{\Gamma} + \mathsf{\Gamma} - q\mathsf{I} \tag{7}$$

By Lipscomb II *et al.* (1988); Dinh & Armstrong (1984); Szeri & Lin (1996); Montgomery-Smith *et al.* (2011), it is known that if $\psi$ was ever isotropic at some time in the past, then

solution to equation (1) is

$$\psi(\mathbf{p}) = \psi_{\mathsf{B}}(\mathbf{p}) = \frac{1}{4\pi(\mathsf{B} : \mathbf{pp})^{3/2}} \tag{8}$$

where $\mathsf{B}$ is a symmetric positive definite matrix with determinant one satisfying

$$\frac{\partial \mathsf{B}}{\partial t} + \mathbf{u} \cdot \boldsymbol{\nabla} \mathsf{B} = -\tfrac{1}{2}\mathsf{B} \cdot (\Omega + \lambda\Gamma) - \tfrac{1}{2}(-\Omega + \lambda\Gamma) \cdot \mathsf{B} \tag{9}$$

Thus from now we will always assume that equation (8) is satisfied.

The 4th order moment tensor $\mathbb{A}$ can be calculated directly from $\mathsf{B}$ using elliptic integrals (Montgomery-Smith *et al.*, 2011) (see also Verleye & Dupret, 1993; VerWeyst, 1998)

$$\mathbb{A} = \mathbb{A}(\mathsf{B}) = \tfrac{3}{4}\int_0^\infty \frac{s\,\mathcal{S}((\mathsf{B} + s\mathsf{I})^{-1} \otimes (\mathsf{B} + s\mathsf{I})^{-1})\,ds}{\sqrt{\det(\mathsf{B} + s\mathsf{I})}} \tag{10}$$

where $\mathcal{S}$ is the symmetrization of a tensor, that is, if $\mathbb{B}$ is a rank $n$ tensor, then $\mathcal{S}(\mathbb{B})_{i_1 \ldots i_n}$ is the average of $\mathbb{B}_{j_1 \ldots j_n}$ over all permutations $(j_1, \ldots, j_n)$ of $(i_1, \ldots, i_n)$.

## 3. A simple one-dimensional example

We will model a fluid between two infinite plates, one at $y = 0$ that is stationary, and one at $y = W$, which is moving in the direction of the $x$-axis at velocity $G$. Thus the average shear strain rate is $G/W$. This gives boundary conditions

$$\mathbf{u}(x, 0, z) = (0, 0, 0), \quad \mathbf{u}(x, W, z) = (G, 0, 0) \tag{11}$$

We assume that $\psi$, and hence $\mathsf{B}$, as a function of $\mathbf{x}$ depends only upon $y$. We also assume that the pressure gradient in the $x$ and $z$ directions is zero, and hence $\boldsymbol{\nabla}\mathbf{u}$, $p$ and $q$ also depend only on $y$. A simple argument shows that if these assumptions are true at $t = 0$, they remain true for $t > 0$.

We will find that it is relatively easy to write a computer program to simulate this behavior. In fact, we will simplify the model even further, and assume that there is an integer $n$ such that $\psi$ is constant on any short interval $W(i-1)/n < y < Wi/n$ $(1 \le i \le n)$. Again, a simple argument shows that if these assumptions are true at $t = 0$, they remain true $t > 0$. And furthermore, it allows us to replace integrals by sums, with the spacial mesh giving exact solutions.

From now on, we will use the following terminology.

(1) The fiber orientation will be called *uniform* if $\psi$ does not depend upon $\mathbf{x}$. That is, all points in the fluid have exactly the same fiber orientation. In particular, $\boldsymbol{\nabla}\psi = 0$.
(2) The fiber orientation will be called *isotropic* if $\psi = 1/4\pi$, that is, the fibers have equal probability of lying in any direction.
(3) The fiber orientation will be called *two dimensional* if (a) $\psi$ does not depend upon $z$, the third component of $\mathbf{x}$, and (b) $\psi(p_1, p_2, p_3) = \psi(p_1, p_2, -p_3)$, that is, the fiber distribution is symmetric about the $xy$-plane.

The reason we call the third situation two-dimensional is that the fiber induces a flow that has no $u_3$ component, and so that fiber orientation and the flow together are symmetric about the $xy$ plane.

Note that $\psi_{\mathsf{B}}$ is uniform if and only if $\mathbf{B}$ does not depend upon $\mathbf{x}$; $\psi$ is isotropic if and only if $\mathsf{B} = \mathsf{I}$; and $\psi$ is two-dimensional if and only $\mathsf{B}$ does not depend upon $z$ and

$$\mathsf{B} = \begin{bmatrix} \mathsf{B}_{11} & \mathsf{B}_{12} & 0 \\ \mathsf{B}_{12} & \mathsf{B}_{22} & 0 \\ 0 & 0 & \mathsf{B}_{33} \end{bmatrix} \tag{12}$$

## 4. A heuristic argument for why 'tumbling' might not take place

To give some physical intuition, let us first describe how small perturbations could have a profound effect on breaking up the periodicity in time of the orientation in the case when $\lambda$ is close but not equal to 1. In this case, Jeffery's equation predicts that the motion of a single fiber in a simple shear is periodic. The fiber spends most of its time in near alignment with the direction of the shear, and then after a fixed amount of time quickly flips almost 180° so that it is again in near alignment.

A reasonable analog is to consider a large number of walkers on a circular track, where a short portion of the track is made of quicksand. We assume that it takes each walker exactly five minutes to complete the part of the track that is not quicksand, and exactly fifty-five minutes to complete the part of the track that is quicksand. Let us suppose that initially there are many walkers spaced equally around the track.

Then at any random time, most of the walkers will be seen to be in the quicksand. However, every hour, and only for a short amount of time, all the walkers will suddenly and seemingly miraculously be equally spaced around the track. And this is in essence what the Jeffery's equation predicts if the initial orientation is isotropic, and $\lambda$ is close but not equal to 1. Most of the time the fibers will be mostly aligned, but every so often, with a period predicted precisely by Jeffery's equation, the fibers will momentarily be isotropic. This is what we refer to as Jeffery's 'tumbling.'

However it is clear that this periodic behavior is rather delicate. For example, suppose that after the first half hour that there is a small earthquake. At this time most of the walkers will be struggling through the quicksand. But the earthquake throws some of them a little bit ahead, and some of them are a little bit behind. Suddenly the delicate timing is lost, and we will lose this periodic behavior where every hour the walkers are equally spaced.

In the same way, if we start with isotropic data and apply Jeffery's equation with $\lambda$ close but not equal to one, and then while the fibers are highly aligned introduce a small perturbation to the fiber distribution, then it is reasonable to suppose that afterwords the 'tumbling' effect will no longer be observed.

We should add that there are other possible reasons why this 'tumbling' might not be seen. For example, one reasonable suggestion is that the fibers all have slightly different aspect ratios.

Finally, we will show in this paper that this intuitive argument does not work as effectively as the author originally hoped. In particular, this argument would seem to apply to two-dimensional distributions. While this turns out to be partially true, the perturbations for two-dimensional fiber orientations grow far less than this description suggests, and to get profound growth of perturbations requires the third dimension in an important way.

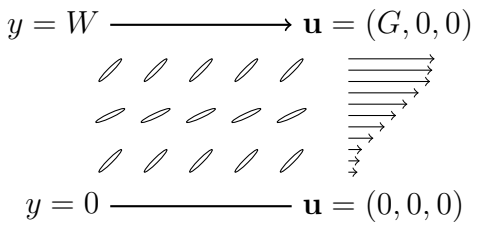


FIGURE 1. Shear flow applied to a non-uniform fiber orientation distribution.

## 5. The solution to the simple one-dimensional example

We show how to compute $\partial \mathsf{B}/\partial t$ from $\mathsf{B}$. First, we obtain $\mathbf{A}$ using equation (10). Now we show how to compute $\boldsymbol{\nabla}\mathbf{u}$.

Equation (6) tells us that $u_2$ is constant, and the boundary conditions (11) tells us that $u_2 = 0$. Equations (5) and (7) become

$$(1 + 2\beta\mathbb{A}_{1122})\frac{\partial u_1}{\partial y} + 2\beta\mathbb{A}_{1223}\frac{\partial u_3}{\partial y} = \Sigma_1 \tag{13}$$

$$2\beta\mathbb{A}_{1222}\frac{\partial u_1}{\partial y} + 2\beta\mathbb{A}_{2223}\frac{\partial u_3}{\partial y} - q = \Sigma_2 \tag{14}$$

$$2\beta\mathbb{A}_{1223}\frac{\partial u_1}{\partial y} + (1 + 2\beta\mathbb{A}_{2233})\frac{\partial u_3}{\partial y} = \Sigma_3 \tag{15}$$

where $\Sigma_1$, $\Sigma_2$, and $\Sigma_3$ are constant with respect to $y$, but are allowed to depend upon $t$. We disregard equation (14), as it tells us the pressure, which is information we do not need.

Setting

$$\mathsf{N} = \mathsf{N}(y) = \begin{bmatrix} 1 + 2\beta\mathbb{A}_{1122} & 2\beta\mathbb{A}_{1223} \\ 2\beta\mathbb{A}_{1223} & 1 + 2\beta\mathbb{A}_{2233} \end{bmatrix} \tag{16}$$

equations (13) and (15) become

$$\begin{bmatrix} \frac{\partial u_1}{\partial y} \\ \frac{\partial u_3}{\partial y} \end{bmatrix} = \mathsf{N}^{-1} \cdot \begin{bmatrix} \Sigma_1 \\ \Sigma_3 \end{bmatrix} \tag{17}$$

and integrating with respect to $y$ from 0 to $W$, we obtain

$$\begin{bmatrix} G \\ 0 \end{bmatrix} = \left( \int_0^W \mathsf{N}^{-1}(\eta)\, d\eta \right) \cdot \begin{bmatrix} \Sigma_1 \\ \Sigma_3 \end{bmatrix} \tag{18}$$

that is,

$$\begin{bmatrix} \Sigma_1 \\ \Sigma_3 \end{bmatrix} = \left( \int_0^W \mathsf{N}^{-1}(\eta)\, d\eta \right)^{-1} \cdot \begin{bmatrix} G \\ 0 \end{bmatrix} \tag{19}$$

and so,

$$\begin{bmatrix} \frac{\partial u_1}{\partial y} \\ \frac{\partial u_3}{\partial y} \end{bmatrix} = \mathsf{N}^{-1} \cdot \left( \int_0^W \mathsf{N}^{-1}(\eta)\, d\eta \right)^{-1} \cdot \begin{bmatrix} G \\ 0 \end{bmatrix} \tag{20}$$

The quantity $\Sigma_1$ is the *shear stress*, that is, the amount of force per unit area of plate exerted in the $x$-direction needed to maintain the constant shear rate $G/W$. Note that if $\psi$ is uniform, then $\Sigma_1 = G/W$, and $\Sigma_3 = 0$.

Now we have a formula for $\boldsymbol{\nabla}\mathbf{u}$, we can compute $\partial\mathsf{B}/\partial t$ using equation (9). Note that the calculations are simplified since it is easily shown that $\mathbf{u}\cdot\boldsymbol{\nabla}\mathsf{B} = 0$.

## 6. Uniform solutions are Periodic

We will give explicit solutions when the fiber orientation is uniform. We will show that the solution is $t_0$-periodic, where

$$t_0 = \frac{4\pi W}{G\sqrt{1-\lambda^2}} \tag{21}$$

and $t_0/2$-periodic if the fiber orientation is two dimensional.

If $\mathsf{B}$ represents a uniform distribution at time $t = 0$, then it can be shown that $\mathsf{B}$ represents a uniform distribution, and $\mathsf{N}$ does not depend upon $y$, for all $t > 0$, and

$$\begin{bmatrix} \frac{\partial u_1}{\partial y} \\ \frac{\partial u_3}{\partial y} \end{bmatrix} = \begin{bmatrix} G/W \\ 0 \end{bmatrix} \tag{22}$$

Hence

$$\tfrac{1}{2}(\Omega + \lambda\Gamma) = \frac{G}{W}\mathsf{D} \tag{23}$$

where

$$\mathsf{D} = \frac{1}{2}\begin{bmatrix} 0 & \lambda+1 & 0 \\ \lambda-1 & 0 & 0 \\ 0 & 0 & 0 \end{bmatrix} \tag{24}$$

that is

$$\frac{\partial \mathsf{B}}{\partial t} = -\frac{G}{W}(\mathsf{B}\cdot\mathsf{D} + \mathsf{D}^T\cdot\mathsf{B}) \tag{25}$$

It may be seen by substitution that the solution is

$$\mathsf{B} = \cdot e^{-t\frac{G}{W}\mathsf{D}^T}\cdot\mathsf{B}(0)\cdot e^{-t\frac{G}{W}\mathsf{D}} \tag{26}$$

Now the eigenvalues of $\mathsf{D}$ are $\pm\frac{i}{2}\sqrt{1-\lambda^2}$, and hence $\mathsf{B}$ is $t_0$-periodic. Furthermore, $e^{-\frac{1}{2}t_0\mathsf{D}} = \mathrm{diag}(-1,-1,1)$, and this commutes with $\mathsf{B}$ if it represents a two-dimensional fiber orientation.

## 7. Analysis of growth of perturbations using linearization

Now let $\mathsf{B}_0$ be a uniform, and hence periodic, solution. Then we can apply the theory of Floquet multipliers (Chicone, 2006, Theorem 2.88). We define the Poincaré map

$$P((\mathsf{B}(0,y))_{0\le y\le W}) = (\mathsf{B}(t_0,y))_{0\le y\le W} \tag{27}$$

The derivative of $P$ around $\mathsf{B} = \mathsf{B}_0$ is called the monodromy map. The idea is to compute the eigenvalues of the derivative . In particular, if we assume that $\mathsf{B}(y)$ is constant on short intervals $W(i-1)/n < y < Wi/n$, then the Poincaré map is a map on a finite dimensional space, and the Floquet theory applies with complete rigor. That is, the differential equation is non-linearly unstable if the monodromy map has any eigenvalues whose absolute value is larger than 1.

In Montgomery-Smith (2011) we have shown the algorithm for computing the eigenvalues of the monodromy map. They are the eigenvalues of $\mathcal{L}(\mathbf{e}_2, t_0)$ as defined in equations (4.1) and (8.3) of Montgomery-Smith (2011). Note there is a sign error in the algorithm: equation (6.10) should read

$$\tilde{\Omega} = i(\hat{\mathbf{u}}\boldsymbol{\kappa} - \boldsymbol{\kappa}\hat{\mathbf{u}}) \tag{28}$$

This sign error makes a huge difference to the numerical results we now give.

Various random values of $\mathsf{B}_0(0)$ were tried. Many of them give a value of the largest absolute value of the eigenvalues that is quite small. But the following matrix gives this value at about 23000 if $\lambda = 0.98$ and $\beta = 10$. Larger values like $\beta = 50$ seemed to cause the program to freeze, suggesting the eigenvalues become very large.

$$\mathsf{B}_0(0) = \begin{bmatrix} 10.7439 & 2.11991 & 3.22009 \\ 2.11991 & 2.93079 & 5.16061 \\ 3.22009 & 5.16061 & 9.15252 \end{bmatrix} \tag{29}$$

If we are only interested in two-dimensional fiber orientations, then we should consider $\mathsf{B}_0(0)$ satisfying $\mathsf{B}_{13}(0) = \mathsf{B}_{23}(0) = 0$, and consider only the top left $3 \times 3$ submatrix of $\mathcal{L}(\mathbf{e}_2, t_0)$. In that case we find that up to numerical precision, the eigenvalues are bounded by one. In the next section, we will prove this by showing that the perturbations grow at most linearly.

## 8. The simple one-dimensional example when the fiber orientation is two-dimensional

In this section we will show that if the fiber orientation is two-dimensional, then two-dimensional perturbations do grow, but only grow at a linear rate. Specifically, we shall show that there is a function $\tau(t, y)$, which we will call the *local time*, such that

$$\mathsf{B} = e^{-\tau \mathsf{D}^T} \cdot \mathsf{B}(0) \cdot e^{-\tau \mathsf{D}} \tag{30}$$

$$\tau(t, y) = \kappa(y)t + O(1) \text{ as } t \to \infty \tag{31}$$

where $\kappa(y)$ depends upon $y$, and in general is non-constant. Note that $\mathsf{B}$ is periodic in $\tau$ with period

$$\tau = \tau_0 = \frac{2\pi}{\sqrt{1 - \lambda^2}} \tag{32}$$

For two-dimensional fiber orientations we have that $\mathbb{A}_{1223} = 0$. Hence $\mathsf{N}(y)$ is a diagonal matrix, and it becomes easy to compute $\mathsf{N}^{-1}(y)$. So equation (20) becomes $\partial u_3/\partial y = 0$ and

$$\frac{\partial u_1}{\partial y} = \left( \int_0^W \frac{dy}{1 + 2\beta \mathbb{A}_{1122}} \right)^{-1} \frac{G}{1 + 2\beta \mathbb{A}_{1122}} \tag{33}$$

This formula can be written as follows. Define

$$\text{Average shear stress} = \Sigma_1 = G \left( \int_0^W \frac{dy}{1 + 2\beta \mathbb{A}_{1122}} \right)^{-1} \tag{34}$$

$$\text{Average shear viscosity} = \left( \frac{1}{W} \int_0^W \frac{dy}{1 + 2\beta \mathbb{A}_{1122}} \right)^{-1} \tag{35}$$

$$\text{Average shear strain rate} = \frac{G}{W} \tag{36}$$

then equation (33) can be restated as

(37) (Average shear stress) = (Average shear viscosity) × (Average shear strain rate)

Note that the average shear viscosity is the harmonic mean of the shear viscosities $1+2\beta\mathbb{A}_{1122}$.

The force per unit area pushing the top and bottom plates in opposite directions is $\Sigma_1$, and since work done is the integral of force with respect to distance, it follows that the energy expended per unit area of plate after time $t$ is given by

$$\int_0^t \Sigma_1 G \, dt \tag{38}$$

We make this quantity dimensionless by dividing by $G$, to give a quantity we call the *normalized energy*

$$E = \int_0^t \Sigma_1 \, dt \tag{39}$$

Note that $E$ is a strictly increasing function of $t$, and $E = 0$ when $t = 0$. Next, we define $\tau$ as the solution to the differential equation

$$\tau = 0 \text{ when } E = 0 \tag{40}$$

$$\frac{\partial \tau}{\partial E} = \frac{1}{1 + 2\beta\mathbb{A}_{1122}} \tag{41}$$

Now

$$\tfrac{1}{2}(\Omega + \lambda\Gamma) = \frac{\partial \tau}{\partial t}\mathsf{D} \tag{42}$$

Hence

$$\frac{\partial \mathsf{B}}{\partial \tau} = -(\mathsf{B} \cdot \mathsf{D} + \mathsf{D}^T \cdot \mathsf{B}) \tag{43}$$

and hence equation (30) follows.

Next, it can be seen that $\partial E/\partial \tau$ and $\mathbb{A} = \mathbb{A}(\mathsf{B})$ are periodic in $E$ with period $E_0$, where

$$E_0 = \int_0^{\tau_0} 1 + 2\beta\mathbb{A}_{1122}(\mathsf{B}(\tau) \, d\tau \tag{44}$$

Notice that $E_0$ is a function only of $\mathsf{B}$ at $t = 0$. Numerical calculations show that $E_0$ depends on $\mathsf{B}(0)$ is a non-trivial manner, that is, different $\mathsf{B}$ at $t = 0$ will, in general, give rise to different values of $E_0$. We show example results of calculations for $\lambda = 0.98$ and $\beta = 50$ in table 1. (Note that we only specify $\mathsf{B}_{11}$, $\mathsf{B}_{12}$, and $\mathsf{B}_{22}$. The other entries are implied by $\mathsf{B}$ representing a two-dimensional fiber orientation, and $\det(\mathsf{B}) = 1$.)

Periodicity implies that

$$\tau = (\tau_0/E_0)E \text{ as } E \to \infty \tag{45}$$

Also, since $1 + 2\beta\mathbb{A}_{1122}$ is a periodic function of $E$ with period $E_0$, we have

$$\int_0^E \frac{dE'}{1 + 2\beta\mathbb{A}_{1122}(\mathsf{B})} = \frac{E}{E_0}\int_0^{E_0} \frac{dE'}{1 + 2\beta\mathbb{A}_{1122}(\mathsf{B})} + O(1) \text{ as } E \to \infty \tag{46}$$

Therefore

$$t = \int_0^E \frac{1}{G}\int_0^W \frac{dy \, dE'}{1 + 2\beta\mathbb{A}_{1122}(\mathsf{B})} = \kappa_1 E + O(1) \text{ as } E \to \infty \tag{47}$$

| $\mathsf{B}_{11}$, $\mathsf{B}_{12}$, $\mathsf{B}_{22}$ | $E_0$ |
|---|---|
| 1.32539, -2.51612, 5.29462 | 124.374 |
| 1.8544, 1.57688, 1.5526 | 140.326 |
| 18.1277, 10.6832, 9.56442 | 43.5925 |
| 3.23236, 1.66221, 0.899942 | 155.327 |
| 5.3305, -4.8482, 5.58189 | 76.7804 |
| 0.768847, -1.6146, 4.90368 | 101.545 |
| 49.6141, -24.1436, 11.7672 | 151.148 |
| 1.04157, 0.660037, 8.18445 | 53.0747 |
| 1.62661, 1.48431, 1.60716 | 138.293 |
| 14.632, 9.25098, 5.85208 | 161.459 |

TABLE 1. Examples of randomly created matrices, and the associated value of $E_0$.

where

$$\kappa_1 = \int_0^W \frac{1}{E_0 G} \int_0^{E_0} \frac{dE'\,dy}{1 + 2\beta \mathbb{A}_{1122}(\mathsf{B})} \tag{48}$$

Thus it can be shown that equation (31) holds with $\kappa = E_0/\tau_0\kappa_1$.

## 9. Results of Simulations

We ran numerical simulations with $\beta = 50$, $G = W = 1$, and $\lambda = 0.98$, and $n = 100$. The ODE is solved using a standard ODE solver, in our case the Runge-Kutta method of order 4 with step size 0.01.

First we considered two-dimensional fiber orientations. In the unperturbed case, we took $\mathsf{B} = \mathsf{I}$ at $t = 0$. In the perturbed case we took

$$\mathsf{B} = \kappa(\mathsf{I} + \epsilon\mathsf{R}) \qquad (t = 0) \tag{49}$$

where $\epsilon = 0.01$ or 0.3, $\mathsf{R}$ is a symmetric matrix whose entries are independent random numbers uniformly chosen in the interval $[-1, 1]$, except that $\mathsf{R}_{13} = \mathsf{R}_{23} = 0$, and $\kappa$ is chosen so that $\det(\mathsf{B}) = 1$.

The plots shown in Figure 2 show the time evolution of shear stress. This is the amount of force per unit area of plate exerted in the $x$-direction, needed to maintain the constant shear rate $G/W = 1$, and is $\Sigma_1$ as defined in equation (13). Note that in the unperturbed case, $\Sigma_1 = 1 + \beta\mathbb{A}_{1122}$. We don't show the perturbed case when $\epsilon = 0.01$ as it looked identical to the unperturbed case.

The plots in Figure 3 show the average over $y$ of the components of $\mathsf{A}$, which are calculated from $\mathsf{B}$ using the formula

$$\mathsf{A} = \tfrac{1}{2} \int_0^\infty \frac{(\mathsf{B} + s\mathsf{I})^{-1}\,ds}{\sqrt{\det(\mathsf{B} + s\mathsf{I})}} \tag{50}$$

We generally prefer reporting shear stress instead of average components of $\mathsf{A}$ is because the former is much easier to measure in experiments (Wang *et al.*, 2008).

Next we considered fiber orientations which are not two-dimensional. In the unperturbed case, we took $\mathsf{B}(0) = \mathsf{B}_0(0)$ as in equation (29). In the perturbed case we took

$$\mathsf{B} = \mathsf{B}_0(0)^{1/2} \cdot \kappa(\mathsf{I} + \epsilon\mathsf{R}) \cdot \mathsf{B}_0(0)^{1/2} \qquad (t = 0) \tag{51}$$

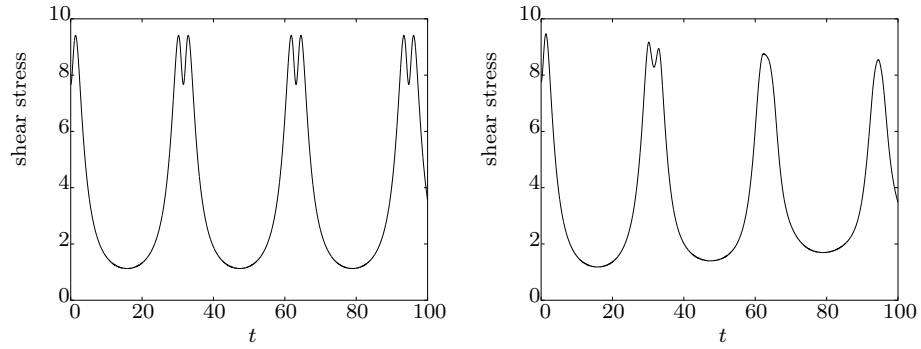


FIGURE 2. Shear stress of shear flows with unperturbed and perturbed fiber orientations.

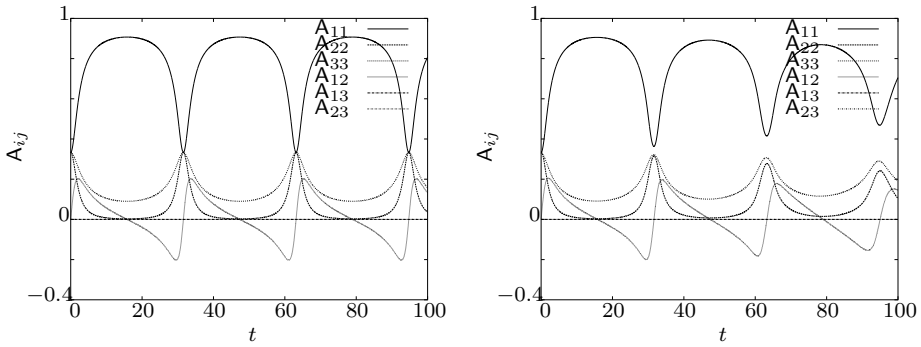


FIGURE 3. Average of components of $\mathsf{A}$ under shear flows with unperturbed and perturbed fiber orientations.

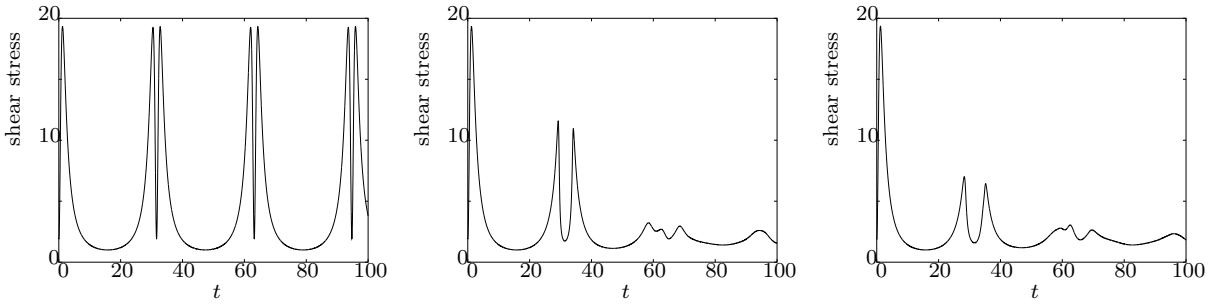


FIGURE 4. Shear stress of shear flows with unperturbed and perturbed fiber orientations.

where $\epsilon = 0.01$ or $0.3$, $\mathsf{R}$ is a symmetric matrix whose entries are independent random numbers uniformly chosen in the interval $[-1, 1]$, and $\kappa$ is chosen so that $\det(\mathsf{B}) = 1$.

The plots shown in Figure 4 show the time evolution of shear stress, and the plots in Figure 5 show the average over $y$ of the components of $\mathsf{A}$, of the unperturbed case, the perturbed case with $\epsilon = 0.01$, and the perturbed case with $\epsilon = 0.3$.

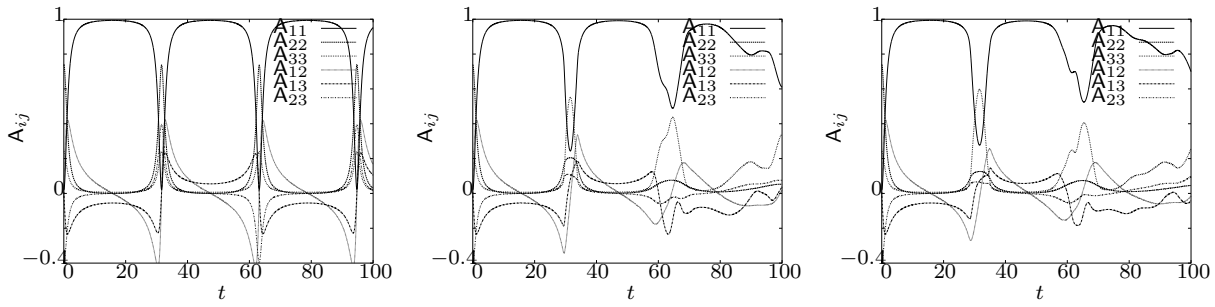


FIGURE 5. Average of components of A under shear flows with unperturbed and perturbed fiber orientations.

## 10. Conclusion

This paper presents results that suggest that the coupling between Jeffery's equation, and Stokes equation when fiber orientation affects viscosity, might be sufficient to account for lack of Jeffery's tumbling in a suspension of fibers in a Newtonian fluid.

The results of this paper should be taken with further caution, since we assumed that all the perturbations depended only on the $y$-variable (that is, they were constant along the invariant planes of the shear flow). It is not clear to the author whether introducing other perturbations will increase or decrease the effect reported here. However asymptotically as $t \to \infty$, non-linear instability has been established.

## 11. Acknowledgments

The author gratefully acknowledge support from N.S.F. grant C.M.M.I. 0727399.

## References

Anczurowski, E. & Mason, S.G. 1967 The kinetics of flowing dispertions iii. equilibrium orientation of rods and discs (experimental). *J. Colloid Int. Sci.* pp. 533–546.

Batchelor, G.K. 1971 Stress generated in a non-dilute suspension of elongated particles by pure straining motion. *Journal of Fluid Mechanics* **46**, 813–829.

Bird, R.B., Curtiss, C.F., Armstrong, R. C. & Hassager, O. 1987 *Dynamics of Polymeric Liquids*, 2nd edn., , vol. 2: Kinetic Theory. New York, NY: John Wiley & Sons, Inc.

Chicone, C. 2006 *Ordinary Differential Equations with Applications*, 2nd edn. New York: Springer-Verlag.

Dinh, S.M. & Armstrong, R.C. 1984 A Rheological Equation of State for Semiconcentrated Fiber Suspensions. *Jn. of Rheology* **28** (3), 207–227.

Folgar, F.P. & Tucker, C.L. 1984 Orientation Behavior of Fibers in Concentrated Suspensions. *Jn. of Reinforced Plastics and Composites* **3**, 98–119.

Jeffery, G.B. 1923 The Motion of Ellipsoidal Particles Immersed in a Viscous Fluid. *Proceedings of the Royal Society of London A* **102**, 161–179.

Lipscomb II, G.G., Denn, M.M., Hur, D.U. & Boger, D.V. 1988 Flow of Fiber Suspensions in Complex Geometries. *Jn. of Non-Newtonian Fluid Mechanics* **26**, 297–325.

Montgomery-Smith, S.J. 2011 Perturbations of the coupled Jeffery-Stokes equations. *J. of Fluid Mechanics* **681**, 622–638.

Montgomery-Smith, S.J., He, Wei, Jack, D.A. & Smith, D.E. 2011 Exact Tensor Closures for the Three Dimensional Jeffery's Equation. *J. of Fluid Mechanics* **680**, 321–335.

Sepehr, M., Carreau, P.J., Grmela, M., Ausias, G. & Lafleur, P.G. 2004 Comparison of Rheological Properties of Fiber Suspensions with Model Predictions. *Jn. of Polymer Engineering* **24** (6), 579–610.

Shaqfeh, E.S.G. & Fredrickson, G.H 1990 The hydrodynamic stress in a suspension. *Physics of Fluids A* **2**, 7–24.

Szeri, A.J. & Lin, D.J. 1996 A deformation tensor model of brownian suspensions of orientable particles —the nonlinear dynamics of closure models. *Journal of Non-Newtonian Fluid Mechanics* **64**, 43–69.

Verleye, V. & Dupret, F. 1993 Prediction of Fiber Orientation in Complex Injection Molded Parts. In *Developments in Non-Newtonian Flows*, pp. 139–163.

VerWeyst, B.E. 1998 Numerical Predictions of Flow Induced Fiber Orientation in Three-Dimensional Geometries. PhD thesis, University of Illinois at Urbana Champaign.

Wang, J., O'Gara, J.F. & Tucker, C.L. 2008 An objective model for slow orientation kinetics in concentrated fiber suspensions: Theory and rheological evidence. *J. Rheology* **52**, 1179–1200.

Department of Mathematics, University of Missouri, Columbia MO 65211, U.S.A.
*E-mail address*: stephen@missouri.edu